Musculoskeletal model-based control interface mimics physiologic hand dynamics during path tracing task

Musculoskeletal model-based control interface mimics physiologic hand dynamics during path tracing task

Dustin L. Crouch, PhD [1], He Huang, PhD [1]

1. UNC-NC State Joint Department of Biomedical Engineering, North Carolina State University, Raleigh, NC, 27695

Corresponding Author
Name: Dustin L. Crouch, PhD
Address: North Carolina State University
1407 Engineering Building 3
911 Oval Drive
Campus Box 7115
Raleigh, NC 27695
Email: dlcrouch@ncsu.edu
Phone: (919) 515-4412
Fax: (919) 515-7760

Keywords: electromyogram, prosthesis control, musculoskeletal model, dynamic simulation, amputation

Word Count: 4776

Abstract:

Objective: We investigated the feasibility of a novel, customizable, simplified EMG-driven musculoskeletal model for estimating coordinated hand and wrist motions during a real-time path tracing task.

Approach: A two-degree-of-freedom (DOF) computational musculoskeletal model was implemented for real-time EMG-driven control of a stick figure hand displayed on a computer screen. After 5 to 10 minutes of undirected practice, subjects were given 3 attempts to trace 10 straight paths, one at a time, with the fingertip of the virtual hand. Able-bodied subjects completed the task on two separate test days.

Main Results: Across subjects and test days, there was a significant linear relationship between log-transformed measures of accuracy and speed (Pearson's $r=0.25$, $p<0.0001$). The amputee subject could coordinate movement between the wrist and MCP joints, but favored metacarpophalangeal joint motion more highly than able-bodied subjects in 8 of 10 trials. For able-bodied subjects, tracing accuracy was lower at the extremes of the model's range of motion, though there was no apparent relationship between tracing accuracy and fingertip location for the amputee. Our result suggests that, unlike able-bodied subjects, the amputee's motor control patterns were not accustomed to the multi-joint dynamics of the wrist and hand, possibly as a result of post-amputation cortical plasticity, disuse, or sensory deficits.

Significance: To our knowledge, our study is one of very few that have demonstrated the real-time simultaneous control of multi-joint movements, especially wrist and finger movements, using an EMG-driven musculoskeletal model, which differs from the many

data-driven algorithms that dominate the literature on EMG-driven prosthesis control. Real-time control was achieved with very little training and simple, quick (~15 second) calibration. Thus, our model is potentially a practical and effective control platform for multifunctional myoelectric prosthesis that could restore more life-like hand function for individuals with upper limb amputation.

Introduction:

There are more than 41,000 individuals in the US who suffer substantial functional impairment as a result of a major upper limb amputation [1]. Despite the emergence of advanced multifunctional prosthetic hands, most commercially-available devices permit users to move only one degree of freedom at a time [2]. Conversely, rotations among joints of the intact limb are often performed simultaneously and continuously to control endpoint (i.e. hand) posture, location, and orientation with remarkable precision and versatility [3]. Simultaneous multi-joint movements are temporally efficient because joint rotations are performed continuously in parallel rather than discretely in series. Enabling effective and coordinated multi-joint prosthesis control for upper limb amputees may enhance function and restore more natural movement ability than conventional controllers.

Several existing algorithms decode multi-joint movement intent directly from motor commands [4-14], i.e. neural signals from the brain or muscles that initiate movement. However, these algorithms do not directly account for the complex interactions between numerous neural, muscular, and skeletal components that

influence motor commands during multi-joint movement. For instance, a muscle's biomechanical contribution to movement depends on its own force output - a non-linear function of its length, shortening velocity, and neural stimulation – as well as the instantaneous active and passive force output of other muscles [15, 16]. Muscles can even influence motion at joints they do not cross [17]. Additionally, since several muscles of the hand are multi-articular, forces generated about the metacarpophalangeal (MCP) joint, for example, are highly dependent on wrist posture [18]. Computational musculoskeletal models, commonly used in biomechanics research, directly incorporate the biomechanical *structure* through which neural stimuli produce movement. Thus, compared to existing algorithms, musculoskeletal models may better account for the many biomechanical factors that influence movements initiated by motor commands.

Musculoskeletal models have been used to predict upper limb kinetics and kinematics from able-bodied electromyograms (EMG) [19-22], but it is unclear whether the same approach is suitable for amputees whose neural and musculoskeletal anatomy and physiology are severely disrupted. Researchers posit that humans employ feedforward motor control based on an internal model of the native limb's dynamic properties that is reinforced by sensory feedback during movement [23-25]. Individuals may retain an internal model of the missing limb after amputation, though its cortical representation may change with deficient or augmented sensory feedback [26, 27]. As a result of the retained internal model, amputees can generate motor commands that are both consistent for a given movement and distinct among different movements. This has been demonstrated by the ability of pattern recognition algorithms, under controlled

experimental conditions, to distinguish among up to 10 wrist and hand movements using EMG recorded from amputees' residual muscles [28] and to distinguish from among 16 intended arm motions using EMG recorded following targeted muscle reinnervation [29-31]. Thus, amputee motor commands reflect movement-specific *biomechanical intent* that, while potentially altered, could be represented in a musculoskeletal model to predict *movement intent* from EMG. When implemented for prosthesis control, such a musculoskeletal model should provide an intuitive interface, behaving as if it were the amputee's own limb. In a previous off-line analysis, we demonstrated that a customized musculoskeletal model could reasonably predict unconstrained (i.e. not task-specific) multi-joint movement from surface EMG for able-bodied subjects and an individual with transradial amputation [32, 33].

The objective of our study was to test whether a customizable musculoskeletal model could enable effective real-time simultaneous multi-joint control of a virtual hand during a path tracing task. More importantly, this model-based EMG interface was tested not only on able-bodied subjects, but also on an individual with a transradial amputation to test the feasibility of our model as a platform for prosthesis control. Our research might lead to a novel method for EMG control of multifunctional artificial arms that produces coordinated motion for functional task performance.

Methods:

The experimental protocol was approved by the University of North Carolina at Chapel Hill Institutional Review Board, and all subjects gave their informed consent to

participate. Five able-bodied subjects (AB1-AB5) with no history of neuromuscular impairment and one individual with a right transradial amputation (subject TRA) participated in the study (Table 1). All subjects were otherwise healthy and had no other chronic health issues (e.g. cardiovascular, cognitive). Subject TRA had no reported pain in the affected limb and qualitatively described a vivid sense of phantom wrist and finger movements.

Model description

We used a planar lumped-parameter musculoskeletal model of the wrist and hand [32, 33] ; the model is described in detail in Appendix A. Briefly, the model included two degrees of freedom, wrist and metacarpophalangeal (MCP) flexion/extension, as prosthesis users have demanded and would benefit from greater wrist movement capability in addition to hand motion [34, 35]. Four Hill-type muscles - one antagonist pair crossing the wrist only and another antagonist pair crossing the wrist and MCP joints - were added to the model. This muscle arrangement was chosen because (1) it is similar the arrangement of muscles that cross the physiologic wrist and MCP joints, and (2) it permitted independent control of wrist and MCP joint movements in both flexion and extension directions. The model was implemented in MATLAB (Mathworks, Inc., MA, USA).

Model Customization

The model was customized for each subject using data from a previous study [32]. In that study, subjects performed isolated and combined wrist and MCP flexion/extension movements. We used an infrared motion capture system (Vicon

Motion Systems Ltd., UK) to record the locations of 9 reflective markers placed on the following anatomical landmarks: lateral and medial humeral epicondyles, radial and ulnar styloid processes, mid-forearm, 2nd and 5th MCP joints, and 2nd and 5th proximal interphalangeal joints. We synchronously recorded electromyograms (EMG) from surface EMG electrodes (Biometrics, Newport, UK) placed over four forearm muscles: extensor digitorum, extensor carpi radialis longus, flexor digitorum, and flexor carpi radialis. These muscles were chosen because the joints they cross, and therefore their biomechanical contributions to movement, are analogous to those of the virtual muscles in the model. For subject TRA, marker locations and EMG were recorded from the sound and amputated limbs, respectively, during mirrored bilateral wrist and hand movements. An inverse kinematics analysis was performed using an upper limb musculoskeletal model [36] in OpenSim [37] to compute joint angles from marker locations. EMG were processed to estimate the muscles' activation state, or force output as a percentage of its maximal force at a given length and shortening velocity [38].

For each test subject, we customized the values of a total of 22 musculoskeletal parameters (5 for uni-articular muscles and 6 for bi-articular muscles) that strongly influenced the force- and joint moment-generating capacity of the muscles in the model: optimal contractile element (CE) length, maximum isometric CE force, *in situ* CE length, parallel elastic element stiffness, and moment arm(s) of each muscle about the joint(s) it crossed. Muscle activation states from EMG recorded in the previous study were applied to the model during a forward dynamic simulation. The 22 musculoskeletal parameters were adjusted iteratively during a constrained global optimization routine

(MATLAB *GlobalSearch* function) to minimize the weighted (2:1 MCP to wrist) sum of squared error between predicted and measured kinematics. Offline analysis in our previous study demonstrated moderate to very high mean correlations (able-bodied Pearson's r: $0.75 \leq r \leq 0.94$; amputee Pearson's r: $0.56 \leq r \leq 0.93$) between measured and customized-model-predicted joint angles during single-joint and simultaneous two-joint movements [32].

Real-time model-based controller

The model was implemented for real-time EMG-driven control in MATLAB (Figure 1). Adhesive bipolar silver/silver chloride surface EMG electrodes with an inter-electrode spacing of 22 mm (Norotrode 20, Myotronics, Inc., WA, USA) were placed approximately over the same four forearm muscles for which EMG was used to optimize the musculoskeletal parameters: extensor digitorum, extensor carpi radialis longus, flexor digitorum, and flexor carpi radialis. EMG signals were recorded at 1000 Hz (Motion Lab Systems, Inc., Louisiana, USA). Data were accumulated in 50 ms blocks in a 1000 ms array for processing to lessen filtering artifacts. The accumulated EMG were high-pass filtered, rectified, low-pass filtered, and downsampled to 100 Hz. EMG from the most recent 50 ms window of the accumulated array were applied to the muscles in the model during a real-time forward dynamic simulation. Based on the applied EMG, muscle forces and the moments they generated about the wrist and MCP joints were computed as described in Appendix A. Given the computed muscle-generated joint moments and previous model states (i.e. joint angles and angular velocities), the model equations of motion were integrated over a 0.01 second timestep to compute the subsequent model states at 100 Hz.

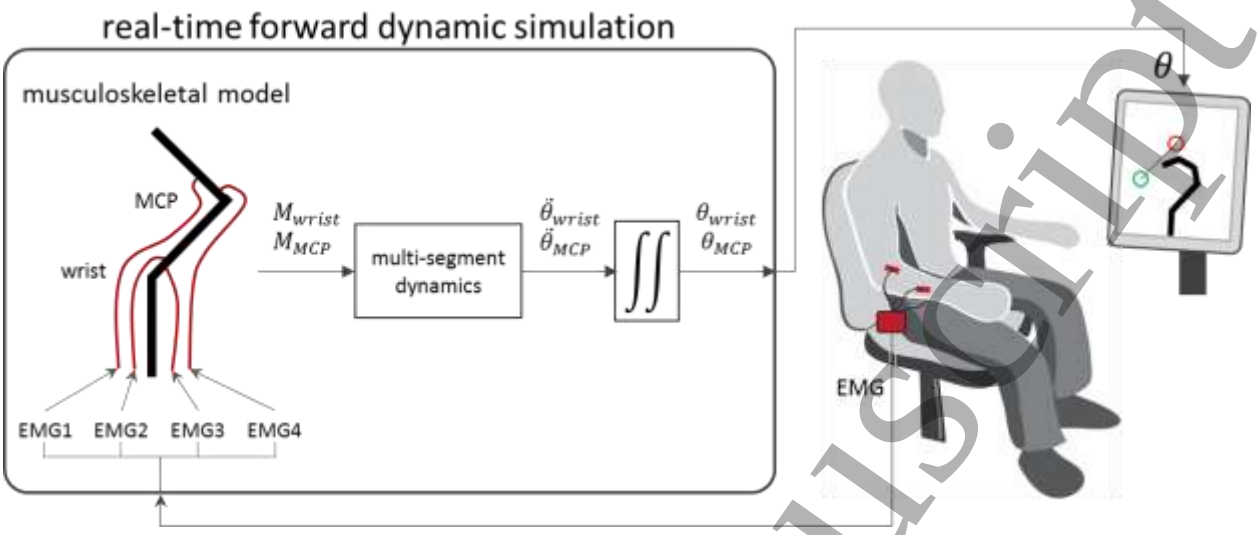

Figure 1: Real-time forward dynamic simulation process and experimental human-computer interface. Processed EMG from four forearm muscles were applied to virtual muscles in the musculoskeletal model. Joint angular accelerations ($\ddot{\theta}$) were computed from the muscle-generated joint moments (M) and multi-segment dynamics equations of motion. The angular accelerations were integrated twice to compute joint angles (θ) which were used to update the posture of a virtual hand displayed on a computer screen directly in front of the seated subject.

The computed model states were used to update the posture of a planar stick figure virtual hand in real-time at 20 Hz. The virtual hand included forearm, palm, and finger segments linked by a wrist and MCP joint. The forearm segment was fixed in a vertical position at the bottom center of the computer screen, while the palm and finger segments were free to rotate about the wrist and MCP joints, respectively. Two joints representing the proximal and distal interphalangeal joints were added distal to the MCP

joint to increase the fingertip's range of motion. The angles of the interphalangeal joints were always equal to the MCP joint angle during real-time control.

Path tracing task

To quantify the control performance enabled by the musculoskeletal model, subjects performed a path tracing task in which they traced straight paths with the fingertip of the virtual hand. The locations and orientations of 10 straight paths, with specified start and end regions, were defined manually to be approximately evenly distributed across the fingertip workspace of the virtual hand (Figure 2). Start and end regions were demarcated by green and red circles, respectively, with a radius of approximately 5% of the total length of the virtual hand from wrist to fingertip. Straight paths were chosen to encourage subjects to coordinate movement of the wrist and MCP joints simultaneously during the task.

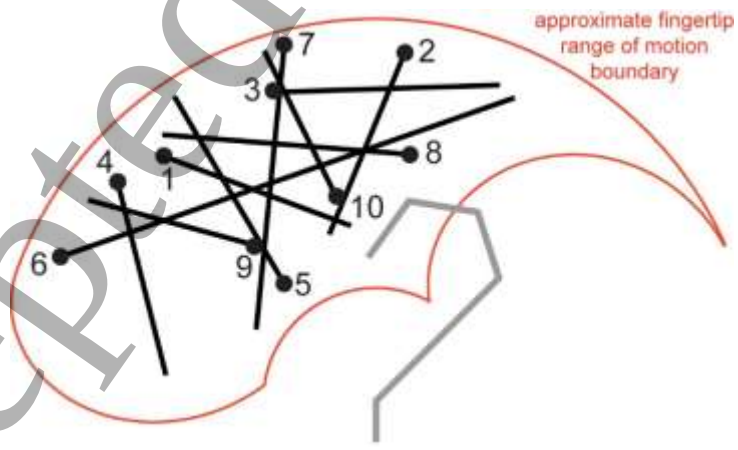

Figure 2: Location and orientation of 10 straight paths that subjects traced during the task relative to the approximate fingertip range of motion (red line) and virtual hand (gray line). The start region is indicated by the black circles.

At the beginning of each test session, subjects were seated directly in front of a computer screen so that they could easily see the virtual hand and target paths displayed on the screen (Figure 1). The arm was supported by the subject with the shoulder and forearm in a neutral posture and the elbow flexed to approximately 90°. EMG was collected briefly (~15 seconds) during maximum voluntary contractions (MVCs) to normalize subsequent EMG during the task. Subjects were given approximately 5 to 10 minutes of undirected practice to become familiar with the control dynamics of the virtual hand. Subjects were then given the following instruction: “Trace each path with the fingertip of the virtual hand as closely as possible while moving from the start to end region as quickly as possible.” The relative importance of these two task goals (accuracy and speed) were left to each subject’s discretion. Subjects traced each path 3 times in succession, and the order of the paths was the same across subjects. A trial was defined from when the fingertip exited the start region to when the fingertip entered the end region. For each trial, we recorded the trial duration, joint angles, fingertip location, and raw and processed EMG.

An important criterion for prosthesis control is whether the model-based controller enabled consistent day-to-day performance. Therefore, able-bodied subjects completed two test sessions on two separate days with the same customized model parameters (EMG during MVCs was re-recorded before each session).

Data Analysis

We quantified subjects' performance in each trial using three measures: mean perpendicular distance, mean fingertip speed, and path efficiency. These parameters correspond approximately to how well subjects controlled the location, speed, and direction, respectively, of the fingertip of the virtual hand during the tracing task. The **mean perpendicular distance (MPD)** between the fingertip and path quantified the accuracy with which subjects traced the paths, where lower MPD indicated greater accuracy. MPD was the perpendicular distance between the fingertip and path averaged across a trial. Perpendicular distance between the fingertip and path trajectory was calculated as (Eq.1):

$$Perpendicular\ Distance = \frac{|a*x_f+b*y_f+c|}{\sqrt{a^2+b^2}} \quad \text{Eq.1}$$

Where x_f and y_f are the x and y coordinates of the fingertip, respectively, and a, b, and c are coefficients of the line defining the straight path (Eq.2).

$$ax + by + c = 0 \quad \text{Eq.2}$$

Mean fingertip speed (S) was the fingertip trajectory length, as a percent of hand length (wrist to fingertip), divided by the trial duration in seconds (Eq.3).

$$S = \frac{fingertip\ trajectory\ length}{trial\ duration} \quad \text{Eq.3}$$

The **path efficiency (PE)** of the fingertip trajectory was computed as a measure of how direct subjects moved the fingertip from the start to the end region (Eq.4) [39].

$$PE = 100\% * \frac{path\ length}{fingertip\ trajectory\ length} \quad \text{Eq.4}$$

Of the 3 trials for each path, the trial with the lowest MPD was selected for further analysis. MPD and S were right skewed; these data were transformed by computing $\log_{10}$(MPD) and $\log_{10}$(S) to allow us to perform statistical tests that assumed normal data distribution.

There is a well-documented tradeoff between speed and accuracy during various tasks [40]. To determine whether a similar tradeoff between these task goals (speed- and accuracy) occurred during the path tracing task, we computed the linear regression of $\log_{10}$(MPD) and $\log_{10}$(S) across all trials, and computed Pearson's correlation coefficient (r) to test the strength of the relationship between the two variables. To estimate how subjects weighted the two task goals in each test session, we grouped $\log_{10}$(MPD) and $\log_{10}$(S) by session, and computed the mean and standard deviation of each variable.

We hypothesized that S and PE, corresponding to the speed and direction of the fingertip, respectively, would influence tracing accuracy. To test this hypothesis, we used able-bodied subjects' data to generate a multiple linear regression model with $\log_{10}$(S) and PE as predictor variables and $\log_{10}$(MPD) as the response variable. The coefficient of multiple determination (R^2) was computed to estimate how much of the variation in $\log_{10}$(S) and PE could explain variation in MPD, a measure of tracing accuracy.

We compared the extent to which able-bodied and amputee subjects simultaneously moved the wrist and MCP joints by computing the ratio of wrist-to-total angular speed ratio (absolute value of angular velocity) at each timepoint during a trial (Eq.5).

$$angular\ speed\ ratio = \frac{|\dot{\theta_w}|-|\dot{\theta_m}|}{|\dot{\theta_w}|+|\dot{\theta_m}|}$$ Eq.5

For each trial, we computed a distribution of the wrist-to-MCP velocity ratio into two bins, dividing timepoints by whether the subject was moving either the wrist or MCP joint faster.

Finally, as the controller was based on a musculoskeletal model, its dynamics were similar to that of the human hand. Specifically, stronger contractions were required to maintain postures near the extremes of the model's range of motion. We plotted MPD as a function of path location to determine whether tracing accuracy may have been influenced by model dynamics.

Statistical comparisons were considered significant for $p \leq 0.05$.

Results

All able-bodied subjects performed the tracing task using their own customized model; parameters were not changed between test sessions. Due to challenges in electrode placement across test sessions, subject TRA performed the tracing task with parameters customized for AB5. The model parameters used by each subject, computed in our previous study, and a video depicting a sample segment of the tracing task experiment accompany the manuscript as Supplementary Data.

All subjects could successfully complete the path tracing task for all paths. Qualitatively, both able-bodied subjects and subject TRA kept the fingertip relatively

close to the target path while moving it from the start to end region (Figure 3). However, tracing performance appeared to differ among paths and subjects.

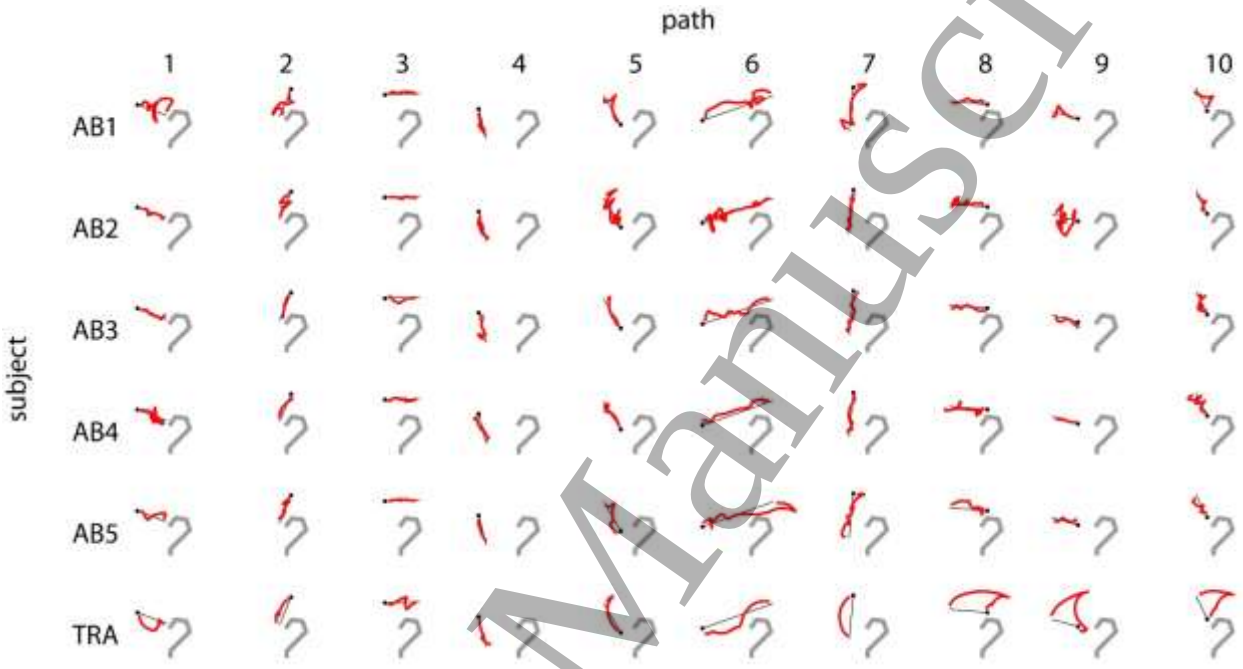

Figure 3: Fingertip trajectories (red line) from trials on test day 1 with the lowest mean perpendicular distance. Target path (black line), start region (black dot), and virtual hand (gray line) shown for reference.

Across trials, tracing accuracy was inversely proportional to the speed with which subjects performed the task. There was a significant linear relationship between $\log_{10}$(MPD) and $\log_{10}$(S) across paths, test days, and subjects (Pearson's r=0.25, p=0.0102, n=108), indicating that the model enabled consistent performance overall. To avoid over-influencing this correlation computation, two outliers were removed (TRA

paths 6 and 7) because the subject traced the paths ballistically at a very high mean fingertip speed (approximately 1.1 and 7.0 hand lengths/sec, respectively); by comparison, the mean and standard deviation of S for all other 108 trials was 0.20 and 0.15 hand lengths/sec, respectively. The linear relationship between $\log_{10}$(MPD) and $\log_{10}$(S) remained significant when only able-bodied subject performance was considered (Pearson's r=0.21, p=0.0387, n=100). When $\log_{10}$(MPD) and $\log_{10}$(S) were averaged within subjects and test sessions, we observed that differences in performance between test sessions could partly be explained by how each subject weighted the two task goals (accuracy and speed) in the session (Figure 4). Thus, subjects weighted the task goals differently from one another, and each AB subject weighted the task goals differently between test days. However, these differences conformed to the overall relationship between accuracy and speed.

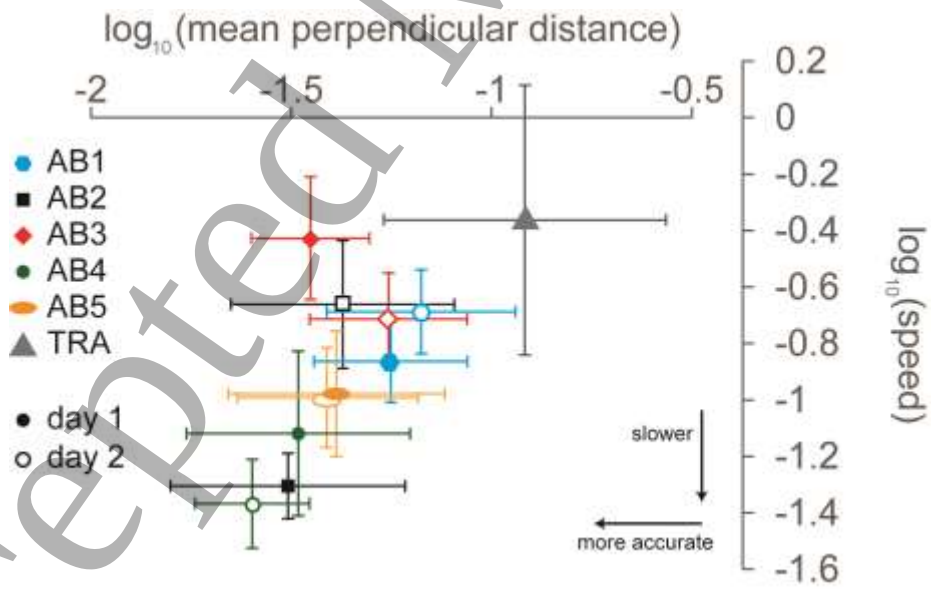

Figure 4: Mean $\log_{10}$(speed) and $\log_{10}$(mean perpendicular distance) for each subject and test day, from trials with the lowest mean perpendicular distance for each path, subject, and test day. Bars indicate +/- 1 standard deviation.

Both $\log_{10}$(S) and PE, related to subjects' control of fingertip speed and direction, respectively, during trials, were significant predictors of $\log_{10}$(MPD), or tracing accuracy. When included as predictor variables of $\log_{10}$(MPD) in a multiple linear regression model, both $\log_{10}$(S) and PE could explain 46% of the variation in $\log_{10}$(MPD) (R^2=0.46, p<0.0001, n=100). By comparison, $\log_{10}$(S) and PE by themselves could only explain 3% (R^2=0.03, p=0.0387, n=100) and 19% (R^2=0.19, p<0.0001, n=100), respectively, of the variation in $\log_{10}$(MPD).

Both AB subjects and TRA could generate coordinated activity among the 4 muscles used to control the virtual hand, which was required to generate the simultaneous, coordinated multi-joint motions needed to trace the paths. For instance, when tracing path 3, subjects AB5 and TRA both generated EMG activity associated with MCP extension and wrist extension that gradually increased over the trial (Figure 5). Similarly, for path 9, subjects AB5 and TRA contracted both MCP extensor and wrist flexor muscles, with some co-contraction of the MCP flexor. That subject TRA could generate coordinate muscle contractions associated with both the wrist and MCP joints is remarkable given that he had no need for or regularly performed muscle contractions to generate multi-joint movements in the more than 2 years since his amputation.

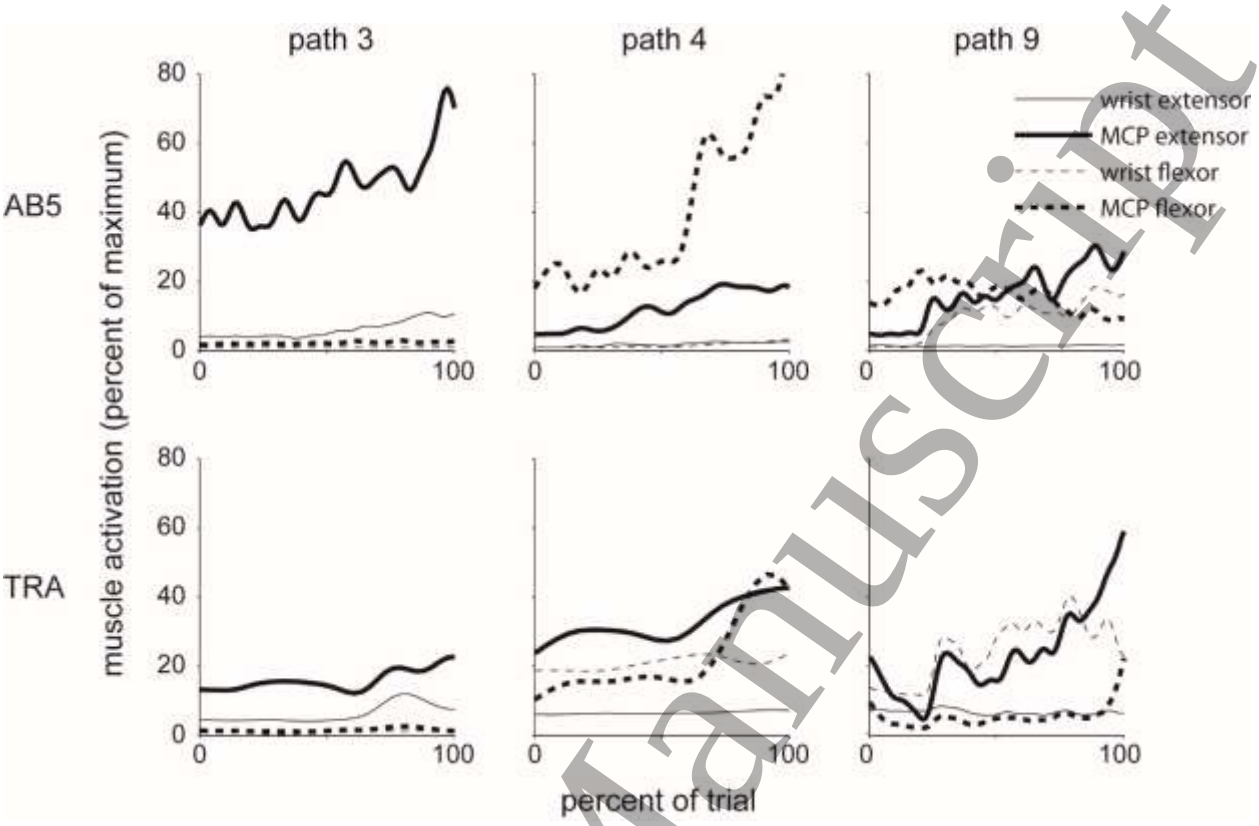

Figure 5: Exemplary post-processed, normalized EMG applied to the model while tracing paths 3, 4, and 9 for subject AB5 (top) and TRA (bottom). EMG shown from trials with the lowest mean perpendicular distance. EMG are labeled by their approximate primary biomechanical action at the wrist and hand.

Despite similarities in muscle coordination while tracing some paths, overall, AB subjects coordinated motion between the wrist and MCP joints differently than subject TRA. Specifically, for 8 of the 10 paths, subject TRA moved the MCP joint faster than the wrist joint *more often* than AB subjects (Figure 6). In other words, subject TRA preferentially favored MCP motion over wrist motion, whereas AB subjects generally moved the wrist and MCP joints equally.

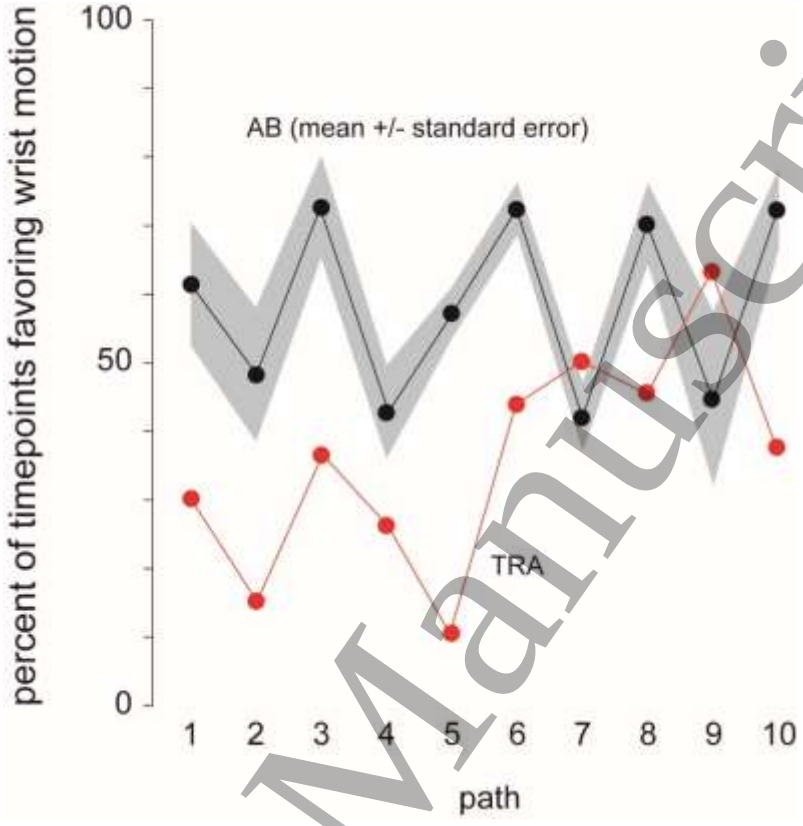

Figure 6: Percentage of trial timepoints in which subjects moved the wrist joint faster than the MCP joint, using kinematic data from trials with the lowest mean perpendicular distance. Subject TRA favored MCP motion over wrist motion more than AB subjects for 8 of 10 target paths.

Finally, MPD, averaged across subjects, was lower toward the middle of the fingertip workspace and higher near the boundaries of the fingertip workspace (Figure 7A). Therefore, subjects could trace paths more accurately within the middle of the model's range of motion, and less accurately at the range of motion extremes. We did not observe a similar relationship between MPD and fingertip location for subject TRA,

which possibly reflects his altered or unfamiliar perception of his hand's dynamic behavior (Figure 7B).

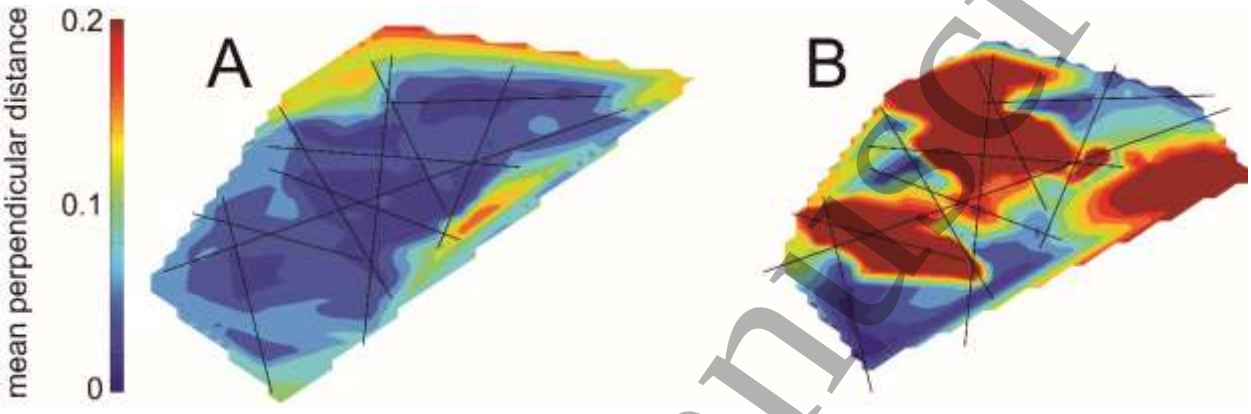

Figure 7: Contour plot of mean perpendicular distance with respect to fingertip location for (A) averaged across able-bodied subjects and test days, and (B) subject TRA. Mean perpendicular distance values were taken from trials with the lowest MPD for each path, subject, and test day. Target paths are shown by black lines.

Discussion

Individuals with upper limb amputations have long demanded prostheses that restore function comparable to that of an intact human limb, and much research continues in pursuit of this goal. One hallmark of intact human limb movement is the ability to coordinate rotations among multiple joints continuously. Our results preliminarily demonstrated that a simplified EMG-driven musculoskeletal hand model can enable effective simultaneous multi-joint control, allowing both able-bodied subjects and an individual with transradial amputation to successfully complete a difficult path

tracing task. The model was quick and simple to calibrate, requiring subjects to generate a few seconds of maximal muscle contractions at the beginning of each test session. The control performance was relatively consistent across subjects, test days, and posture, except at extreme postures. Subjects achieved this performance with very little training, indicating that the model provides an intuitive control interface. Subjects' overall performance, including the tradeoff between speed and accuracy, accuracy's dependence on joint posture, and the intuitiveness of the interface, all suggest that the model's dynamic properties are closely aligned with those of the human hand. This is no surprise since the model directly incorporates the limb's biomechanical structures that dictate its dynamic behavior.

Qualitatively, fingertip trajectories for some paths and subjects were noisy due to erroneous oscillatory fingertip motion. Since model kinematics were predicted from EMG-driven muscle forces, motion errors were likely associated with EMG generation, recording, and processing. For instance, EMG signals are notoriously nonstationary even for isokinetic or isometric tasks, indicating physiologic variability of motor commands [41]. EMG was recorded during dynamic movements which, along with other sources, can introduce low-frequency noise [42]. Methods used to filter and normalize EMG can greatly influence the variability of subsequent muscle force estimates across timepoints. Additional development is needed to identify experimental, signal processing, or modeling techniques that will mitigate the effects of unintended EMG variability on endpoint motion.

Tracing accuracy was inversely proportional to the speed with which subjects completed the task, a phenomenon that has been well-characterized for human task

performance and human-computer interfaces and reflected in the well-known Fitts' law model [40]. Other algorithms intended for upper limb prosthesis control have been shown to conform to Fitts' law [9, 39, 43, 44]. Our study did not include such a Fitts' law style test for two reasons. First, Fitts' law assumes that the movements subjects are required to generate during the task are "highly overlearned" [40]. Since one of the study goals was to demonstrate that our model-based controller was intuitive, we intentionally did not allow subjects to practice the task, much less to the point that it was overlearned. Second, the dynamic response of each subject's customized model was similar to, but did not exactly match, their own (perceived) limb movements. Therefore, we expect that some training and practice will improve tracing performance such that a Fitts' law style test would be appropriate. In future studies, we plan to conduct such a test to permit more direct, standardized comparison between our model and other control algorithms.

Subject TRA in our study, and amputees in several others, have reported a sensation of voluntary phantom limb movement. However, as reported in other studies [10], TRA also had difficulty imagining or generating appropriate muscle contractions for simultaneous multi-joint movement. Because our musculoskeletal model mimics the dynamics of the intact human hand, it provides physiologic visual feedback of the imagined movements to the user. Previous studies have shown that visual feedback matching imagined movements can enhance activity in the primary motor cortex and reduce phantom limb pain [45], and that training enhances prosthesis functional performance [46]. Thus, we expect that our model would provide amputees appropriate

feedback of their hand movements and, with retraining, improved ability to control multi-joint movements.

Several algorithms have been developed and tested to interpret simultaneous multi-joint movements from motor commands measured either directly from the brain or from EMG. For instance, neural signals recorded by implanted electrode arrays have allowed users to control the endpoint (hand) location and posture (e.g. grasp) of a multi-degree-of-freedom robotic arm [4-6]. Algorithms used to decode movement intent from EMG for upper limb prostheses include artificial neural networks [7, 8], support vector regression [9], principal component analysis [10], nonnegative matrix factorization [11], pattern recognition [12], Kalman filter prediction [14], and linear regression [13]. Though we expect that our musculoskeletal model may generate more physiologic movement predictions than these algorithms, it is unclear how they would compare in terms of task performance. More online testing is needed to quantify and compare performance among these control approaches.

Though our model enables both wrist and MCP flexion/extension, few commercially-available prosthetic terminal devices include active wrist flexion/extension. However, there is strong demand by amputees for prostheses with greater wrist motion [34]. A number of upper limb tasks, including feeding/drinking, hair combing, opening a jar, and pouring from a jug, require wrist flexion/extension motions [3, 47]. Restricted wrist flexion/extension motion in able-bodied subjects led to poorer performance during standard clinical hand function tests [48]. Additionally, absence of prosthetic wrist flexion induced compensatory motions at proximal joints in amputees that could increase injury risk or fatigue [35, 48, 49].

A key requirement of independently controlling multiple joints is recording distinct, individually-modulated neural commands from several independent muscle sources. EMG recorded from the forearm is subject to crosstalk, especially when using surface EMG electrodes, given the close proximity of many muscles that contribute to several different wrist and hand movements [50]. In able-bodied subjects, recording EMG from the muscles required to control our model is relatively straightforward since they are all anatomically superficial in some part of the forearm. However, placing surface EMG electrodes for individuals with transradial amputation is more challenging because muscles that contribute to finger movement, for instance, are deep to muscles that contribute to wrist movement in the proximal residual forearm. We faced this challenge for subject TRA in this study, leading us to use a model customized for another subject instead if TRA's own model during the tracing task. To mitigate this challenge in future studies, we plan to use intramuscular fine-wire electrodes to more reliably record muscle-specific EMG signals in transradial amputees. Signal processing techniques that distinguish EMG and eliminate crosstalk may also be useful [51].

Another important requirement for clinical applications of myoelectric control systems is robustness to electrode shift [52]. Across test sessions, electrodes used to measure EMG were placed over approximately the same muscles as determined by manual palpation and photographs of electrode locations from a previous test session. Though electrode locations may have differed across test sessions, subjects, given the real-time visual feedback of the virtual hand movements, could have adapted to this variation by generating different muscle contractions. Permanently implanted electrodes

[53] are highly attractive for our model-based controller because they stabilize electrode location while providing muscle-specific EMG signals over a long period of time.

Limitations

There were several limitations of our study to consider. First, we tested a small and unequal number of able-bodied and amputee participants. The study was designed to test the feasibility of our musculoskeletal model as a potential platform for prosthesis control, rather than directly compare performance or neuromuscular behavior between able-bodied and amputee subjects. We plan to include more amputee subjects in future studies to test the broad applicability of our model-based control across the patient population.

We used a simplified hand model that does not incorporate all biomechanical structures that influence hand dynamics. Offline, the model predicted subjects' wrist and MCP kinematics reasonably well, but with some error [32, 33]. These prediction errors may have undermined performance of the virtual task, but online prosthesis testing is needed to determine how these errors may disrupt real-world task performance.

Movements of the interphalangeal joints were approximated in the virtual hand by matching their joint angles to the MCP joint angle. This allowed us to test our model-based control over a larger fingertip workspace. However, this inter-joint coupling is not necessarily physiologic as these joints can be actuated independently from the MCP joint by other intrinsic and extrinsic hand muscles [54]. Thus, the coupling may distract subjects if the movements of the virtual hand and their own hand differ.

Since the model was customized for each able-bodied subject, its dynamics and range of motion differed among subjects. Though all subjects could move the fingertip to all path locations, it may have been more difficult for some subjects to reach some locations depending on their model's dynamics and range of motion. Thus, intra-subject differences in model dynamics likely caused differences in task performance.

We did not directly compare virtual task performance between our model-based controller and other algorithms, as other studies have done [13, 43, 44]. Given major differences between virtual and prosthetic interfaces, the value of comparing control algorithms based on virtual task performance is uncertain. For instance, our virtual path tracing task required very precise control of fingertip location, which may not be a requirement for some daily living tasks, such as grasping. Using a prosthesis adds mass to the distal forearm, which will influence EMG recorded from residual upper limb muscles. Prosthesis control may suffer from EMG variability due to electrode shift, limb posture, and fatigue [55, 56], conditions that may be less prevalent during a virtual task.

Conclusion

In conclusion, our study is one of few to demonstrate real-time simultaneous multi-joint control of wrist and finger movements based on a musculoskeletal model. With very little training, subjects could complete a complex path tracing task, suggesting that our model could potentially enable effective multi-joint control of multifunctional myoelectric prostheses. Though our results are promising, more work is needed to implement the model for prosthesis control and test users' performance of daily living tasks, especially

under varying conditions of fatigue, arm posture, and grasped object weight, among others. Additionally, we will include more individuals with amputation to evaluate whether the model could enable consistent, effective control performance across the clinical population. By representing the perceived biomechanics of an amputee's limb, we expect our model could potentially restore more natural, biomimetic movement control of multifunctional prosthetic hands.

Acknowledgements

This work was sponsored by the Defense Advanced Research Projects Agency (DARPA) Biological Technologies Office (BTO) Hand Proprioception and Touch Interfaces (HAPTIX) program under the auspices of Dr. Doug Weber through the DARPA Contracts Management Office Grant/Contract No. N66001-16-2-4052. This project was also supported by NSF #1527202, DHHS/NIDILRR #90IF0064, and DOD #OR140147 & #13014002.

References

[1] K. Ziegler-Graham, E. J. MacKenzie, P. L. Ephraim, T. G. Travison, and R. Brookmeyer, "Estimating the prevalence of limb loss in the United States: 2005 to 2050," *Arch Phys Med Rehabil,* vol. 89, pp. 422-9, Mar 2008.

[2] A. Fougner, O. Stavdahl, P. J. Kyberd, Y. G. Losier, and P. A. Parker, "Control of upper limb prostheses: terminology and proportional myoelectric control-a review," *IEEE Trans Neural Syst Rehabil Eng,* vol. 20, pp. 663-77, Sep 2012.

[3] C. J. v. Andel, N. Wolterbeek, C. A. M. Doorenbosch, D. Veeger, and J. Harlaar, "Complete 3D kinematics of upper extremity functional tasks," *Gait Posture,* vol. 27, pp. 120-127, 2008.

[4] M. S. Fifer, G. Hotson, B. A. Wester, D. P. McMullen, Y. Wang, M. S. Johannes*, et al.*, "Simultaneous neural control of simple reaching and grasping with the modular prosthetic limb using intracranial EEG," *IEEE Trans Neural Syst Rehabil Eng,* vol. 22, pp. 695-705, May 2014.

[5] B. Wodlinger, J. E. Downey, E. C. Tyler-Kabara, A. B. Schwartz, M. L. Boninger, and J. L. Collinger, "Ten-dimensional anthropomorphic arm control in a human brain-machine interface: difficulties, solutions, and limitations," *J Neural Eng,* vol. 12, p. 016011, Feb 2015.

[6] T. Yanagisawa, M. Hirata, Y. Saitoh, H. Kishima, K. Matsushita, T. Goto*, et al.*, "Electrocorticographic control of a prosthetic arm in paralyzed patients," *Ann Neurol,* vol. 71, pp. 353-361, Mar 2012.

[7] A. Ameri, E. J. Scheme, E. N. Kamavuako, K. B. Englehart, and P. A. Parker, "Real-time, simultaneous myoelectric control using force and position-based training paradigms," *IEEE Trans Biomed Eng,* vol. 61, pp. 279-87, Feb 2014.

[8] S. Muceli and D. Farina, "Simultaneous and proportional estimation of hand kinematics from EMG during mirrored movements at multiple degrees-of-freedom," *IEEE Trans Neural Syst Rehabil Eng,* vol. 20, pp. 371-378, May 2012.

[9] A. Ameri, E. N. Kamavuako, E. J. Scheme, K. B. Englehart, and P. A. Parker, "Support vector regression for improved real-time, simultaneous myoelectric control," *IEEE Trans Neural Syst Rehabil Eng,* vol. 22, pp. 1198-209, Nov 2014.

[10] D. Yatsenko, D. McDonnall, and K. S. Guillory, "Simultaneous, proportional, multi-axis prosthesis control using multichannel surface EMG," *Conf Proc IEEE Eng Med Biol Soc,* vol. 2007, pp. 6134-6137, 2007.

[11] N. Jiang, K. B. Englehart, and P. A. Parker, "Extracting simultaneous and proportional neural control information for multiple-DOF prostheses from the surface electromyographic signal," *IEEE Trans Biomed Eng,* vol. 56, pp. 1070-1080, Apr 2009.

[12] A. J. Young, L. H. Smith, E. J. Rouse, and L. J. Hargrove, "Classification of simultaneous movements using surface EMG pattern recognition," *IEEE Trans Biomed Eng,* vol. 60, pp. 1250-1258, May 2013.

[13] L. H. Smith, T. A. Kuiken, and L. J. Hargrove, "Evaluation of Linear Regression Simultaneous Myoelectric Control Using Intramuscular EMG," *IEEE Trans Biomed Eng,* vol. 63, pp. 737-746, Apr 2016.

[14] E. Okorokova, M. Lebedev, M. Linderman, and A. Ossadtchi, "A dynamical model improves reconstruction of handwriting from multichannel electromyographic recordings," *Front Neurosci,* vol. 9, p. 389, 2015.

[15] F. E. Zajac, "Muscle and tendon: properties, models, scaling, and application to biomechanics and motor control.," *Critical Rev Biomed Eng,* vol. 17, pp. 359-411, 1989.

[16] A. Vandenberghe, L. Bosmans, J. De Schutter, S. Swinnen, and I. Jonkers, "Quantifying individual muscle contribution to three-dimensional reaching tasks," *Gait Posture,* vol. 35, pp. 579-584, Apr 2012.

[17] F. E. Zajac and M. E. Gordon, "Determining muscle's force and action in multi-articular movement," *Exerc Sport Sci Rev,* vol. 17, pp. 187-230, 1989.

[18] R. Savage, "The influence of wrist position on the minimum force required for active movement of the interphalangeal joints," *J Hand Surg Br,* vol. 13, pp. 262-268, Aug 1988.

[19] K. Manal, R. V. Gonzalez, D. G. Lloyd, and T. S. Buchanan, "A real-time EMG-driven virtual arm," *Comput Biol Med,* vol. 32, pp. 25-36, Jan 2002.

[20] E. K. Chadwick, D. Blana, A. J. van den Bogert, and R. F. Kirsch, "A real-time, 3-D musculoskeletal model for dynamic simulation of arm movements," *IEEE Trans Biomed Eng,* vol. 56, pp. 941-948, Apr 2009.

[21] J. Langenderfer, S. LaScalza, A. Mell, J. E. Carpenter, J. E. Kuhn, and R. E. Hughes, "An EMG-driven model of the upper extremity and estimation of long head biceps force," *Comput Biol Med,* vol. 35, pp. 25-39, Jan 2005.

[22] T. K. Koo and A. F. Mak, "Feasibility of using EMG driven neuromusculoskeletal model for prediction of dynamic movement of the elbow," *J Electromyogr Kinesiol,* vol. 15, pp. 12-26, Feb 2005.

[23] D. M. Wolpert and J. R. Flanagan, "Motor prediction," *Curr Biol,* vol. 11, pp. R729-R732, Sep 18 2001.

[24] R. Shadmehr and F. A. Mussa-Ivaldi, "Adaptive representation of dynamics during learning of a motor task," *J Neurosci,* vol. 14, pp. 3208-3224, May 1994.

[25] M. Kawato, "Internal models for motor control and trajectory planning," *Curr Opin Neurobiol,* vol. 9, pp. 718-727, Dec 1999.

[26] J. P. Dewald and R. F. Beer, "Abnormal joint torque patterns in the paretic upper limb of subjects with hemiparesis," *Muscle Nerve,* vol. 24, pp. 273-83, Feb 2001.

[27] C. Mercier, K. T. Reilly, C. D. Vargas, A. Aballea, and A. Sirigu, "Mapping phantom movement representations in the motor cortex of amputees," *Brain,* vol. 129, pp. 2202-2210, Aug 2006.

[28] G. Li, A. E. Schultz, and T. A. Kuiken, "Quantifying pattern recognition-based myoelectric control of multifunctional transradial prostheses," *IEEE Trans Neural Syst Rehabil Eng,* vol. 18, pp. 185-192, Apr 2010.

[29] H. Huang, P. Zhou, G. Li, and T. A. Kuiken, "An analysis of EMG electrode configuration for targeted muscle reinnervation based neural machine interface," *IEEE Trans Neural Syst Rehabil Eng,* vol. 16, pp. 37-45, Feb 2008.

[30] P. Zhou, M. Lowery, A. D. J, and T. Kuiken, "Towards Improved Myoelectric Prosthesis Control: High Density Surface EMG Recording After Targeted Muscle Reinnervation," *Conf Proc IEEE Eng Med Biol Soc,* vol. 4, pp. 4064-7, 2005.

[31] P. Zhou, M. M. Lowery, K. B. Englehart, H. Huang, G. Li, L. Hargrove*, et al.*, "Decoding a new neural machine interface for control of artificial limbs," *J Neurophysiol,* vol. 98, pp. 2974-82, Nov 2007.

[32] D. L. Crouch and H. Huang, "Lumped-Parameter Electromyogram-Driven Musculoskeletal Hand Model: A Potential Platform For Real-Time Prosthesis Control," *J Biomech,* vol. 49, pp. 3901-3907, 2016.

[33] D. L. Crouch and H. Huang, "Musculoskeletal model predicts multi-joint wrist and hand movement from limited EMG control signals," *Conf Proc IEEE Eng Med Biol Soc,* pp. 1132-1135, 2015.

[34] E. Biddiss and T. Chau, "Upper-limb prosthetics: critical factors in device abandonment," *Am J Phys Med Rehabil,* vol. 86, pp. 977-987, Dec 2007.

[35] F. Montagnani, M. Controzzi, and C. Cipriani, "Is it Finger or Wrist Dexterity That is Missing in Current Hand Prostheses?," *IEEE Trans Neural Syst Rehabil Eng,* vol. 23, pp. 600-609, Jul 2015.

[36] K. R. Saul, X. Hu, C. M. Goehler, M. Daly, M. E. Vidt, A. Velisar*, et al.*, "Benchmarking of dynamic simulation predictors in two software platforms using an upper limb musculoskeletal model.," *Computer Methods in Biomechanics and Biomedical Engineering,* vol. 18, pp. 1445-1458, 2015.

[37] S. L. Delp, F. C. Anderson, A. S. Arnold, P. Loan, A. Habib, C. T. John*, et al.*, "OpenSim: Open-Source Software to Create and Analyze Dynamic Simulations of Movement," *IEEE Transactions on Biomedical Engineering,* vol. 54, pp. 1940-1950, 2007.

[38] D. G. Lloyd and T. F. Besier, "An EMG-driven musculoskeletal model to estimate muscle forces and knee joint moments in vivo," *Journal of Biomechanics,* vol. 36, pp. 765-776, Jun 2003.

[39] M. R. Williams and R. F. Kirsch, "Evaluation of head orientation and neck muscle EMG signals as command inputs to a human-computer interface for individuals with high tetraplegia," *IEEE Trans Neural Syst Rehabil Eng,* vol. 16, pp. 485-496, Oct 2008.

[40] P. M. Fitts, "The information capacity of the human motor system in controlling the amplitude of movement," *J Exp Psychol,* vol. 47, pp. 381-391, Jun 1954.

[41] E. Shwedyk, R. Balasubramanian, and R. N. Scott, "A nonstationary model for the electromyogram," *IEEE Trans Biomed Eng,* vol. 24, pp. 417-424, Sep 1977.

[42] C. J. De Luca, L. D. Gilmore, M. Kuznetsov, and S. H. Roy, "Filtering the surface EMG signal: Movement artifact and baseline noise contamination," *J Biomech,* vol. 43, pp. 1573-1579, May 28 2010.

[43] S. M. Wurth and L. J. Hargrove, "A real-time comparison between direct control, sequential pattern recognition control and simultaneous pattern recognition control using a Fitts' law style assessment procedure," *J Neuroeng Rehabil,* vol. 11, p. 91, 2014.

[44] A. J. Young, L. H. Smith, E. J. Rouse, and L. J. Hargrove, "A comparison of the real-time controllability of pattern recognition to conventional myoelectric control for discrete and simultaneous movements," *J Neuroeng Rehabil,* vol. 11, p. 5, 2014.

[45] P. Giraux and A. Sirigu, "Illusory movements of the paralyzed limb restore motor cortex activity," *Neuroimage,* vol. 20 Suppl 1, pp. S107-11, Nov 2003.

[46] A. W. Dromerick, C. N. Schabowsky, R. J. Holley, B. Monroe, A. Markotic, and P. S. Lum, "Effect of training on upper-extremity prosthetic performance and motor learning: a single-case study," *Arch Phys Med Rehabil,* vol. 89, pp. 1199-204, Jun 2008.

[47] A. Murgia, P. J. Kyberd, P. H. Chappell, and C. M. Light, "Marker placement to describe the wrist movements during activities of daily living in cyclical tasks," *Clin Biomech (Bristol, Avon),* vol. 19, pp. 248-254, Mar 2004.

[48] B. D. Adams, N. M. Grosland, D. M. Murphy, and M. McCullough, "Impact of impaired wrist motion on hand and upper-extremity performance," *J Hand Surg Am,* vol. 28, pp. 898-903, Nov 2003.

[49] T. Bertels, T. Schmalz, and T. Ludwigs, "Objectifying the Functional Advantages of Prosthetic Wrist Flexion," *J Prosthet Orthot,* vol. 21, pp. 74-78, 2009.

[50] J. P. Mogk and P. J. Keir, "Crosstalk in surface electromyography of the proximal forearm during gripping tasks," *J Electromyogr Kinesiol,* vol. 13, pp. 63-71, Feb 2003.

[51] J. M. Kilner, S. N. Baker, and R. N. Lemon, "A novel algorithm to remove electrical cross-talk between surface EMG recordings and its application to the measurement of short-term synchronisation in humans," *J Physiol,* vol. 538, pp. 919-930, Feb 1 2002.

[52] A. J. Young, L. J. Hargrove, and T. A. Kuiken, "The effects of electrode size and orientation on the sensitivity of myoelectric pattern recognition systems to electrode shift," *IEEE Trans Biomed Eng,* vol. 58, pp. 2537-2544, Sep 2011.

[53] P. F. Pasquina, M. Evangelista, A. J. Carvalho, J. Lockhart, S. Griffin, G. Nanos*, et al.*, "First-in-man demonstration of a fully implanted myoelectric sensors system to control an advanced electromechanical prosthetic hand," *J Neurosci Methods,* vol. 244, pp. 85-93, Apr 15 2015.

[54] E. Y. S. Chao, K. N. An, W. P. Cooney III, and R. L. Linscheid, *Biomechanics of the Hand: A Basic Research Study*. Singapore: World Scientific, 1989.

[55] D. Tkach, H. Huang, and T. A. Kuiken, "Study of stability of time-domain features for electromyographic pattern recognition," *J Neuroeng Rehabil,* vol. 7, p. 21, 2010.

[56] Y. Geng, P. Zhou, and G. Li, "Toward attenuating the impact of arm positions on electromyography pattern-recognition based motion classification in transradial amputees," *J Neuroeng Rehabil,* vol. 9, pp. 2-11, 2012.